



A Thiazole-Based Polymer Donor for Efficient Organic Solar Cells

Ye Xu^{1,2} · Huifeng Yao¹ · Tao Zhang^{1,2} · Lijiao Ma¹ · Jianhui Hou^{1,2}

Received: 23 March 2022 / Revised: 7 April 2022 / Accepted: 8 April 2022 / Published online: 9 June 2022
© The Author(s) 2022

Abstract

The development of new materials plays a critical role in improving the efficiency of organic solar cells (OSCs). At present, the relatively high-lying highest occupied molecular orbital (HOMO) level of the high-efficiency polymer donor is regarded as one of the main reasons for the low open-circuit voltage (V_{oc}). In this work, we introduced the strong electron-withdrawing thiazole unit into the construction of a polymer donor. We designed and prepared an alternating donor–acceptor material, namely PSZ, by copolymerizing 4-methyl thiazole with an electron-donating benzodithiophene unit and studied its application in high-efficiency OSCs. The optical and electrical properties of the new material were characterized by UV–Vis absorption spectroscopy and electrochemical cyclic voltammetry. Results show that PSZ is a typical wide-bandgap material with a high optical bandgap of 2.0 eV and a deep HOMO level of -5.70 eV. When a non-fullerene BTP-eC9 was selected as the acceptor material, V_{oc} reached 0.88 V in the resulting device, and the corresponding power conversion efficiency (PCE) was 8.15%. In addition, when PSZ was added as the third component to the binary photoactive combination with PBDB-TF as the donor and BTP-eC9 as the acceptor, V_{oc} of the cell device could be increased, thereby obtaining a high PCE of 17.4%. These results indicated that introducing thiazole units into polymer donors can remarkably reduce the HOMO levels and improve V_{oc} and PCE in OSCs.

Keywords Organic solar cells · Energy conversion efficiency · Polymer donor · Thiazole unit

Introduction

Organic solar cells (OSCs) are a new type of photovoltaic technology that uses organic semiconductors to convert solar energy into electricity. The intrinsic characteristics of organic semiconductors endow OSCs with many outstanding advantages, such as lightweight, flexibility, and colors [1]. In recent years, the development of new materials has boosted the power conversion efficiency (PCE) of OSCs up to 19% [2], showing great potential in practical applications. Different from traditional inorganic materials such as crystal silicon, organic semiconductors have low

dielectric constants. The absorption of solar photons generates tightly bound excitons (electron–hole pairs) instead of free carriers. The photoactive layers of OSCs usually adopt a bulk-heterojunction structure, which is composed of donors and acceptors with different electronegativities to convert photogenerated excitons into free carriers. The photovoltaic performance of OSCs is closely related to the photoresponse range, energy level arrangement, aggregation morphology, and charge transport properties of the materials [3]. First, the donor and acceptor should have complementary absorption spectra to match with the solar spectrum to fully absorb solar photons, which is crucial for obtaining excellent short-circuit current density (J_{sc}). Second, the maximum value of the open-circuit voltage (V_{oc}) is limited by the difference between the highest occupied molecular orbital (HOMO) energy level of the donor and the lowest unoccupied molecular orbital (LUMO) energy level of the acceptor. In addition, appropriate HOMO–HOMO and LUMO–LUMO differences are necessary for efficient charge separation. Therefore, controlling the molecular energy level of photovoltaic materials is important. Finally, suppressing the recombination, improving the charge mobility

✉ Huifeng Yao
yaohf@iccas.ac.cn

✉ Jianhui Hou
hjhzzl@iccas.ac.cn

¹ State Key Laboratory of Polymer Physics and Chemistry, Institute of Chemistry, Chinese Academy of Sciences, Beijing 100190, China

² University of Chinese Academy of Sciences, Beijing 100049, China

of materials, and optimizing the blended morphology are also necessary to improve the transport of charge carriers [4], which can improve the fill factors (FF) of cell devices. In recent years, the development of new donor and acceptor materials has greatly improved OSC efficiency [5–8]. In 2015, Zhan et al. [9] reported non-fullerene acceptor ITIC, which demonstrated good photovoltaic performance. Subsequently, non-fullerene materials gradually replaced fullerene derivatives as the main acceptors in high-efficiency OSCs. At present, most highly efficient devices are prepared from Y6-like non-fullerene acceptors as reported by Zou et al. [10]. For donor materials, related studies have shown that polymers with a solution pre-aggregation effect can easily form a phase-separated morphology in an interpenetrating network with non-fullerene acceptors, which can promote efficient charge transport, thereby obtaining excellent photovoltaic efficiency. For example, the polymer PBDB-T and its derivatives, including PBDB-TF [11], J51 series [12], P2F-EHp [13], and PBQx [14] (Fig. 1), can achieve outstanding photovoltaic performances with non-fullerene acceptors. Among the derivatives, PBDB-TF is widely used in the construction of high-efficiency photovoltaic cells. Recently, we combined it with the Y6 derivative, namely, BTP-eC9, and achieved a high PCE of more than 17% [15, 16]. Considering that J_{sc} and FF parameters of photovoltaic cells in this system are close to the theoretical maximum value, further, improvement becomes challenging. However, the energy loss of the cell device during photoelectric conversion is relatively large, and V_{oc} is only approximately 0.83–0.84 V. Therefore, V_{oc} could still be improved by rational molecular design.

Theoretically, downshifting the HOMO of the donor or upshifting the LUMO of the acceptor are two important molecular design strategies to increase V_{oc} . In this work, we

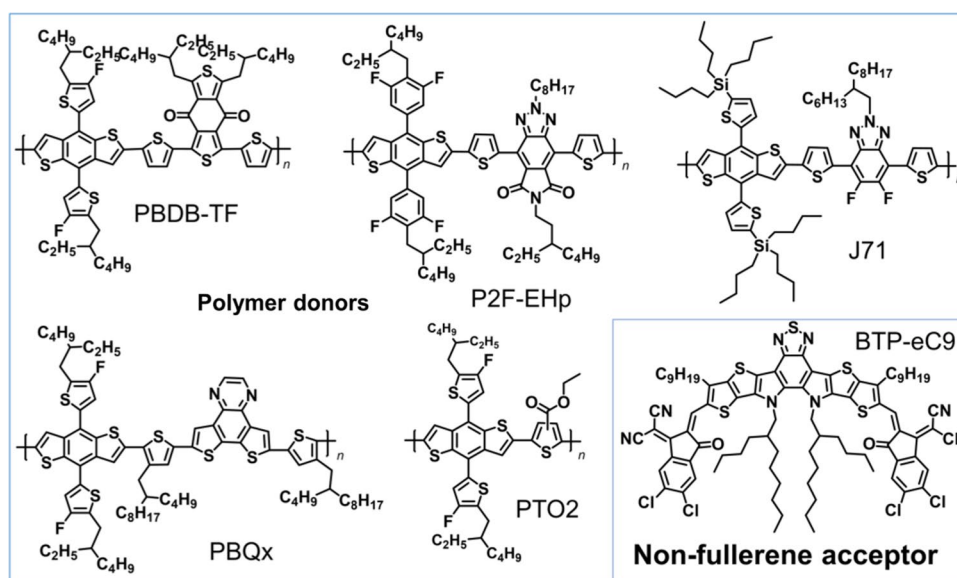
investigated the application of thiazole units in designing deep HOMO-level donors by copolymerizing 4-methyl thiazole as an electron-withdrawing acceptor, which contains a typical donor unit, with fluorinated thienyl-benzodithiophene (F-BDT). In addition, we designed and synthesized a polymer, namely PSZ. This polymer has a high optical band-gap of 2.0 eV and an HOMO level of -5.70 eV. The results of temperature-dependent absorption spectra indicated that the polymer had a solution pre-aggregation effect, which can promote the formation of a good phase-separated morphology in the active layer. When blended with non-fullerene acceptor BTP-eC9 to fabricate photovoltaic devices, V_{oc} of 0.88 V was obtained with PCE of 8.15%. Moreover, when PSZ was used as the third component (20%, w/w) in PBDB-TF:BTP-eC9 binary cell, V_{oc} of the device increased to 0.85 V, and a high PCE of 17.4% could be obtained. These results indicated that the introduction of thiazole into the conjugated backbone of the donor can reduce the HOMO energy level of the material, which can improve V_{oc} , thereby fabricating high-efficiency OSCs.

Results and Discussion

Design and Preparation of the Polymer Material

The development of polymer donors plays a crucial role in improving the efficiency of OSCs. For three decades, a wide variety of building units and polymer materials with excellent photovoltaic properties have been reported. Among them, benzodithiophene with a two-dimensional conjugated thiophene side chain (2D-BDT) is regarded as an outstanding donor unit because of its large conjugated plane, strong electron-rich property, and excellent hole transportability.

Fig. 1 Chemical structures of representative donor and acceptor materials



At present, the relatively high-lying HOMO energy levels of 2D-BDT-based donor materials limit the V_{oc} values of corresponding photovoltaic devices. Therefore, downshifting the HOMO levels of such polymers is necessary. Thiazoles are a class of five-membered heterocycles containing nitrogen and sulfur, and the relatively high electronegativity of the nitrogen atom endows the unit with an electron-withdrawing property. In addition, its simple structure can be used to replace the complex moieties in the construction of organic photovoltaic materials, which can reduce the synthetic cost of the final material. Given the abovementioned characteristics, we combined fluorinated 2D-BDT (BDT-Sn) with 4-methyl thiazole-bromine (Sz-Br) to design an alternating copolymer PSZ.

Density Functional Theory Calculations

We first performed theoretical calculations for the polymer on the B3LYP/6-31G (d, p) level using Gaussian based on density functional theory [17]. As shown in Fig. 2, we used two repeating units as the model to represent the polymer to reduce the calculation cost, where long alkyl side chains in the structure were also replaced by methyl groups. Figure 2a shows the optimized molecular conformation, where we can find that the BDT has different twist angles when it is attached to both sides of the thiazole: the methyl side is 9.2° , whereas the nitrogen atom side is only 1.4° and 0.5° . The polymer has good planarity, which is important for the formation of ordered intermolecular arrangements, thereby improving the charge transport property.

Figure 2b shows the molecular electrostatic potential map, from which the delocalization of electrons in the conjugated backbone can be intuitively understood [18]. First, the electrostatic potential of the main chain composed of BDT and thiazole is relatively continuous, which should

be closely related to the intramolecular electron push–pull interaction. The negative electrostatic potential value indicates the donor nature of the polymer. In addition, BDT has a lower electrostatic potential than thiazole, and the region with the smallest electrostatic potential appears at the link between the nitrogen atom and thiophene in BDT. Figure 2c, d shows the calculated LUMO and HOMO distributions, both of which show continuous characteristics, and the calculated energy levels are -2.46 and -5.19 eV, respectively. Notably, the calculated HOMO energy level of the PSZ model is lower than that of PBDB-TF under the same conditions, which is consistent with our molecular design strategy and is expected to obtain higher V_{oc} in photovoltaic cells.

Preparation of Polymers

The polymer PSZ was prepared via a traditional Stille coupling reaction (Fig. 3). The detailed procedures were as follows: equivalents of BDT-Sn and 4-methyl thiazole-bromine (Sz-Br) were used as monomers (0.3 mmol); tetrakis triphenylphosphine palladium ($\text{Pb}(\text{PPh}_3)_4$) was used as catalyst (15 mg), and toluene was used as solvent (9 mL); the reaction was heated at 110°C for 18 h under the protection of argon atmosphere; after the reaction solution was cooled, it was precipitated in methanol solvent (50 mL) and filtered, and then the polymer was purified using a Soxhlet extractor; the final chloroform phase was concentrated and precipitated in methanol again; after being filtered, it was dried in a vacuum oven for more than 10 h before use. Given the asymmetric nature of 4-methyl thiazole and the unselective coupling reaction of 2,5 bromine with BDT-Sn, the final polymer PSZ should have two kinds of linking models.

Fig. 2 Calculated results for the polymer. **a** Optimized molecular conformation, **b** molecular electrostatic potential map, **c** calculated LUMO, and **d** HOMO distributions

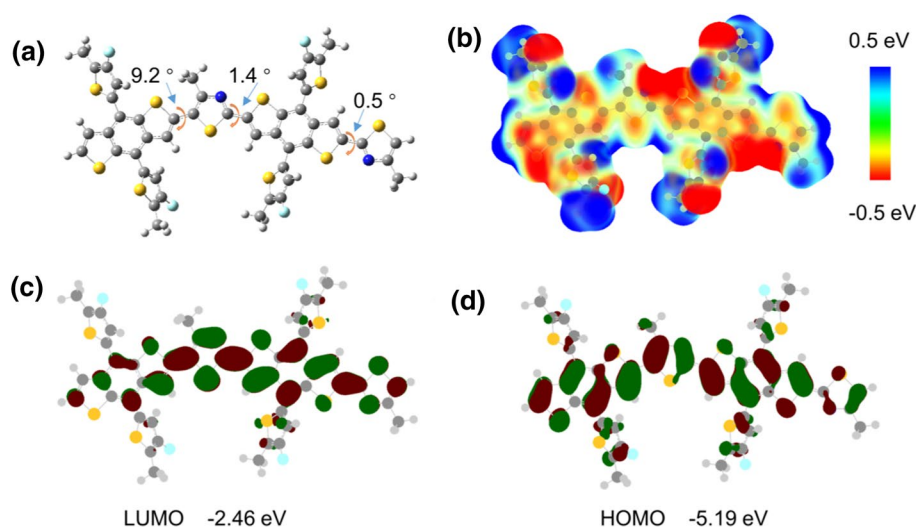
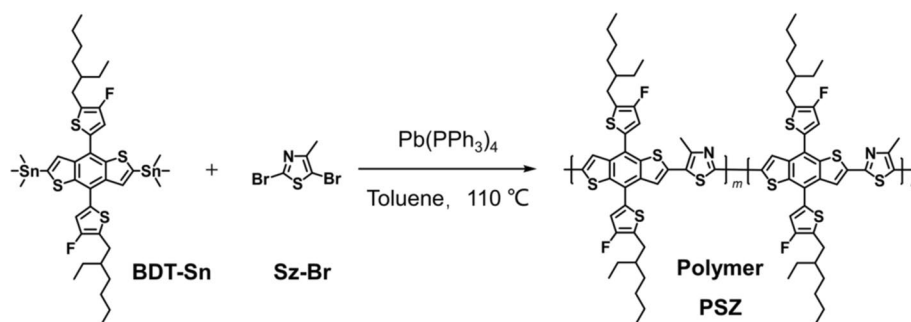


Fig. 3 Fabrication of PSZ

Fundamental Optoelectronic Properties

The fundamental properties of materials, such as the absorption spectrum, molecular energy levels, and aggregation behavior, greatly affect their performance in photovoltaic cells. In this study, we first characterized the temperature-dependent UV–Vis absorption spectra of the polymer in the solution state and its absorption in the thin-film state. In addition, we used cyclic voltammetry to study the electrochemical energy levels of the polymer thin film.

Absorption Spectrum

Figure 4a shows the absorption spectrum of PSZ in chlorobenzene. The main absorption range of the polymer covers 300–600 nm, and the absorption peak is located at 526 nm. When increasing the solution temperature, the absorption spectrum undergoes a clear blue shift, and the intensity of the shoulder peak at the long-wavelength (561 nm) gradually decreases. This phenomenon indicates that PSZ has a solution pre-aggregation effect, which is similar to many high-efficiency polymer donors, thereby forming good phase-separated morphologies when blending with non-fullerene acceptors.

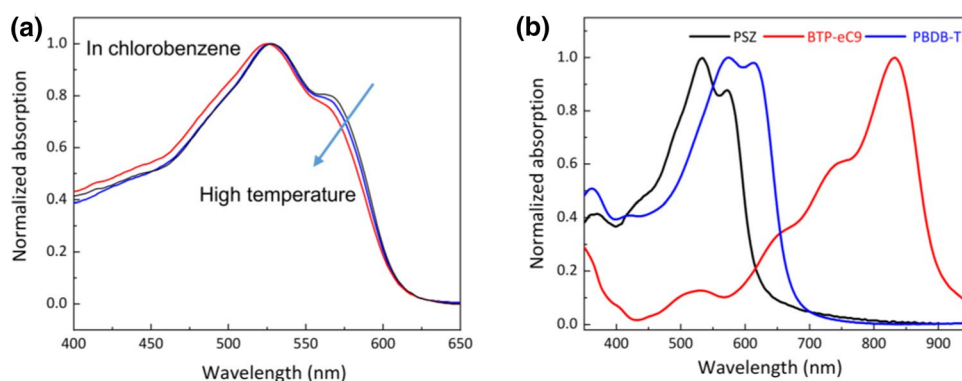
Figure 4b displays the absorption spectrum of PSZ as a thin film. From solution to thin-film states, the main absorption peak has a redshift by 9 nm, and the intensity of the shoulder peak at the long-wavelength is enhanced. This

finding indicates that the polymer formed an ordered intermolecular arrangement during film formation. Calculated based on the absorption onset (619 nm), the optical band gap of PSZ is approximately 2.0 eV, indicating that PSZ is a typical wide-bandgap material. Here we also provided the absorption spectra of the polymer donor PBDB-T and the non-fullerene acceptor BTP-eC9 for comparison. The main absorption bands of the three materials show good complementarity. Blending PSZ with BTP-eC9 or adding PSZ to the combination of PBDB-TF and BTP-eC9 can utilize the solar photons from 300 to 900 nm.

Energy Levels of Polymer Materials

Using an electrochemical workstation (CHI650D), we measured the ionization potential of the polymer PSZ film by the three-electrode method. In the measurement, glassy carbon, platinum wire, and silver electrodes were used as working, counter, and reference electrodes, respectively. 0.1 mol/L acetonitrile solution of tetrabutylammonium hexafluorophosphate was used as an electrolyte, and the test results were corrected by the ferrocene (Fc/Fc^+) redox potentials. Based on the voltage–current curve shown in Fig. 5, the ionization potential of PSZ was -5.70 eV (corresponding to the HOMO energy level in the theoretical calculation), which is an important value in polymer donors, and the result is consistent with the theoretical calculation. These results indicate that the polymer may obtain high- V_{oc} photovoltaic cells.

Fig. 4 Absorption spectra of the materials. **a** Temperature-dependent absorption spectra of the polymer PSZ in chlorobenzene; **b** absorption spectra of the thin films of PSZ, PBDB-TF, and BTP-eC9



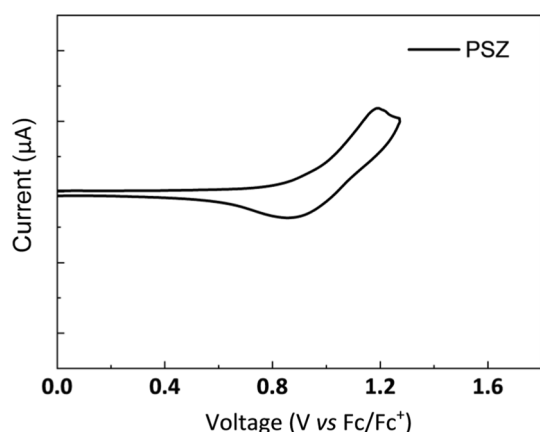


Fig. 5 Electrochemical characterization of the polymer thin film

Fabrication and Characterization of Photovoltaic Cells

In addition to the photoactive layer, the device structure of OSC also includes anodes, cathodes, and interface layers. In this work, indium tin oxide (ITO) was used as the transparent conductive anode, PEDOT:PSS as the anode interface layer, PDINN as the cathode interfacial layer, and silver as the cathode. Traditional device configuration with ITO/PEDOT:PSS/active layer/PDINN/Ag structure was fabricated. Cell devices were prepared as follows: the cleaned ITO electrodes were treated with ultraviolet ozone on a clean bench, and then the PEDOT:PSS solution was spin-coated onto ITO with a thickness of ~10 nm, followed by baking treatment at 150 °C for 15 min. After being transferred into the glove box, the mixed solution of donor and acceptor (the ratio of donor: acceptor was 1:1.2; the polymer concentration was 7.5 mg/mL, and chloroform:1,8-diiodooctane [1:0.5%, v/v] were used as processing solvents) was coated onto PEDOT:PSS. The active layer was approximately 100 nm thick. The interface layer PDINN was spin-coated onto the active layer, and the Ag electrode was evaporated under vacuum conditions to obtain a complete photovoltaic device. We characterized the photovoltaic performance of

the cells using a 3A solar simulator, which was calibrated using a standard silicon cell before testing. First, we prepared the device by blending the polymer PSZ with BTP-eC9 as the photoactive layer. Then, we added PSZ as the third component into the mixture of PBDB-TF:BTP-eC9 to prepare ternary devices.

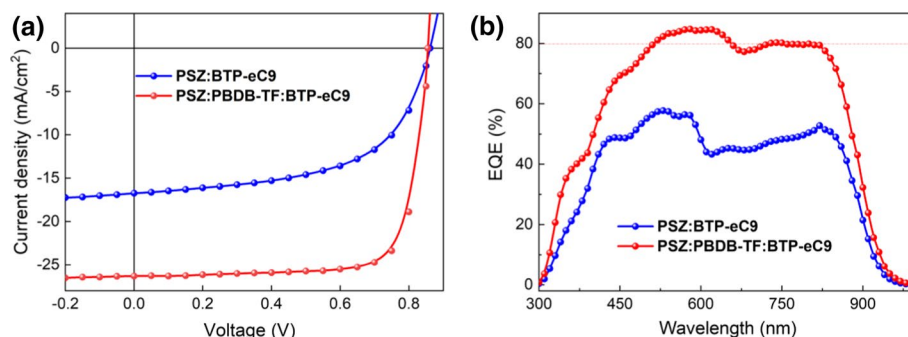
Characteristics of Voltage–Current (J–V)

During preparation, the ratio of donor: acceptor in the active layer, the types of solvents and additives, thermal annealing, and other treatment processes remarkably affect the performance of the device. In this work, we optimized the abovementioned processing conditions to obtain optimal photovoltaic parameters. Figure 6a shows the voltage–current curves of the optimized binary and ternary photovoltaic cells, and the detailed photovoltaic parameters are listed in Table 1. The cell device based on PSZ:BTP-eC9 achieved V_{oc} of 0.88 V. This value is higher than most of the cell devices with PBDB-TF as the donor material, which is primarily attributed to the deep energy level of PSZ. The J_{sc} value of the device was 17.8 mA/cm², which is not a high value for a cell with a photoresponse range of approximately 900 nm. The result indicates that many photogenerated excitons in the system are not effectively dissociated, or severe charge recombination occurred; thus, only a few electrons were collected by the electrode, which was also related to the lower FF (0.52) of the cell device. Based on the energy levels of PSZ and BTP-eC9, the HOMO energy levels are close, which is unfavorable for the dissociation of photogenerated excitons, and it may be related to the moderate J_{sc} and FF. Finally, the cell device based on the PSZ:BTP-eC9 obtains a PCE of 8.15%.

Table 1 Photovoltaic parameters of devices

Devices	V_{oc} (V)	J_{sc} (mA/cm ²)	FF	PCE (%)
PSZ:BTP-eC9	0.88	17.8	0.52	8.15 (8.08 ± 0.06)
PSZ:PBDB-TF:BTP-eC9	0.85	26.3	0.78	17.4 (17.2 ± 0.2)

Fig. 6 **a** Voltage–current curves, **b** EQE curves for photovoltaic cells



Although the binary photovoltaic cell prepared by the combination of PSZ and non-fullerene acceptor BTP-eC9 did not achieve a high PCE, V_{oc} of the device is quite prominent. Therefore, we tried to add it as the third component to the highly efficient PBDB-TF:BTP-eC9. Given the previous experience [19], we controlled the content of PSZ to 20% of PBDB-TF, where the overall donor–acceptor ratio remained unchanged. A ternary component photovoltaic cell was prepared. The binary device based on PBDB-TF:BTP-eC9 was also investigated, and the detailed photovoltaic parameters were as follows: V_{oc} of 0.84 V, J_{sc} of 25.9 mA/cm², FF of 0.78, and PCE of 17.0%. Small variances were still observed when compared with the results of our previous report, which should be related to the different device configurations and polymer batches used. In addition, we found that V_{oc} of the ternary cell device was 0.85 V, which was lower than that of the binary device based on PSZ:BTP-eC9, but it showed a slight improvement compared with the PBDB-TF:BTP-eC9 device. J_{sc} and FF of the ternary cell were 26.3 mA/cm² and 0.78, respectively. The PCE of ternary cell devices was 17.4%, which is among the top results in single-junction OSCs. By contrast, improved V_{oc} should be associated with the downshift of the HOMO level, and the slightly increased J_{sc} may be related to the enhanced absorption in the short-wavelength region.

External Quantum Efficiency

Figure 6b shows the external quantum efficiency (EQE) curves of binary and ternary photovoltaic cells. Both devices showed photoresponse from 300 to 900 nm. The EQE values of the binary device based on PSZ:BTP-eC9 were lower than 60%, and the corresponding integrated current density was 16.2 mA/cm². The relatively low EQE values indicated that the overall efficiency from photogenerated excitons to output electrons in this system was not high. By contrast, the EQE value of the ternary cell device had a significant increase in the whole response range, and most of the regions were above 80%. The highest value reached 85% at 620 nm, and the integrating current density was 25.5 mA/cm². The variances among the values obtained from the voltage–current curves and EQEs were within 5%, which confirmed the reliability of the testing.

Charge Mobility

Charge transport plays an important role in the performance of photovoltaic cells. We used the linearly increased photo-induced charge extraction (photo-CELIV) technology to study the fast carrier mobility of cell devices. Combined with the curves shown in Fig. 7, the carrier mobilities of binary PSZ:BTP-eC9 and ternary PSZ:PBDB-TF:BTP-eC9 devices were calculated to be 2.4×10^{-4} and 1.2×10^{-4} cm²/

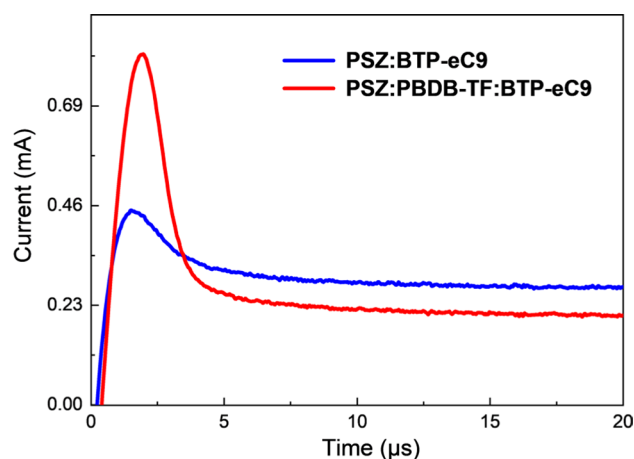


Fig. 7 Measurement of faster charge carrier mobility in working devices

(V·s), respectively. The binary device had slightly higher mobility than the ternary device, but the difference was not significant.

Blend Morphology

The morphology of the donor–acceptor blend has a direct impact on charge transport and recombination. A phase-separated interpenetrating network with an appropriate phase scale is necessary for obtaining high efficiency. We investigated the surfaces of binary and ternary blend films by atomic force microscopy (AFM). Based on the height images shown in Fig. 8a, c, both active layers have smooth and flat surfaces, and the root mean square surface roughness (R_q) of the binary and ternary films is quite close, which are 1.48 nm and 1.49 nm, respectively. Based on the phase images (Fig. 8b, d), both films have fiber-like phase-separated morphologies with appropriate domain sizes, which may be related to the solution pre-aggregation of polymers PSZ and PBDB-TF.

Conclusion

In this work, we studied the application of the thiazole unit in designing highly efficient polymer donors. We designed and prepared alternating copolymer PSZ by copolymerizing 4-methyl thiazole with benzodithiophene, and we explored the photovoltaic performance of the polymer in binary and ternary OSCs. Polymer PSZ is a typical wide-bandgap material with an optical bandgap of 2.0 eV, and its HOMO level is -5.70 eV. When blending with the non-fullerene acceptor BTP-eC9, V_{oc} of 0.88 V and a PCE of 8.15% were achieved. When PSZ was added as the third component into the PBDB-TF and BTP-eC9-based binary system, V_{oc} can be

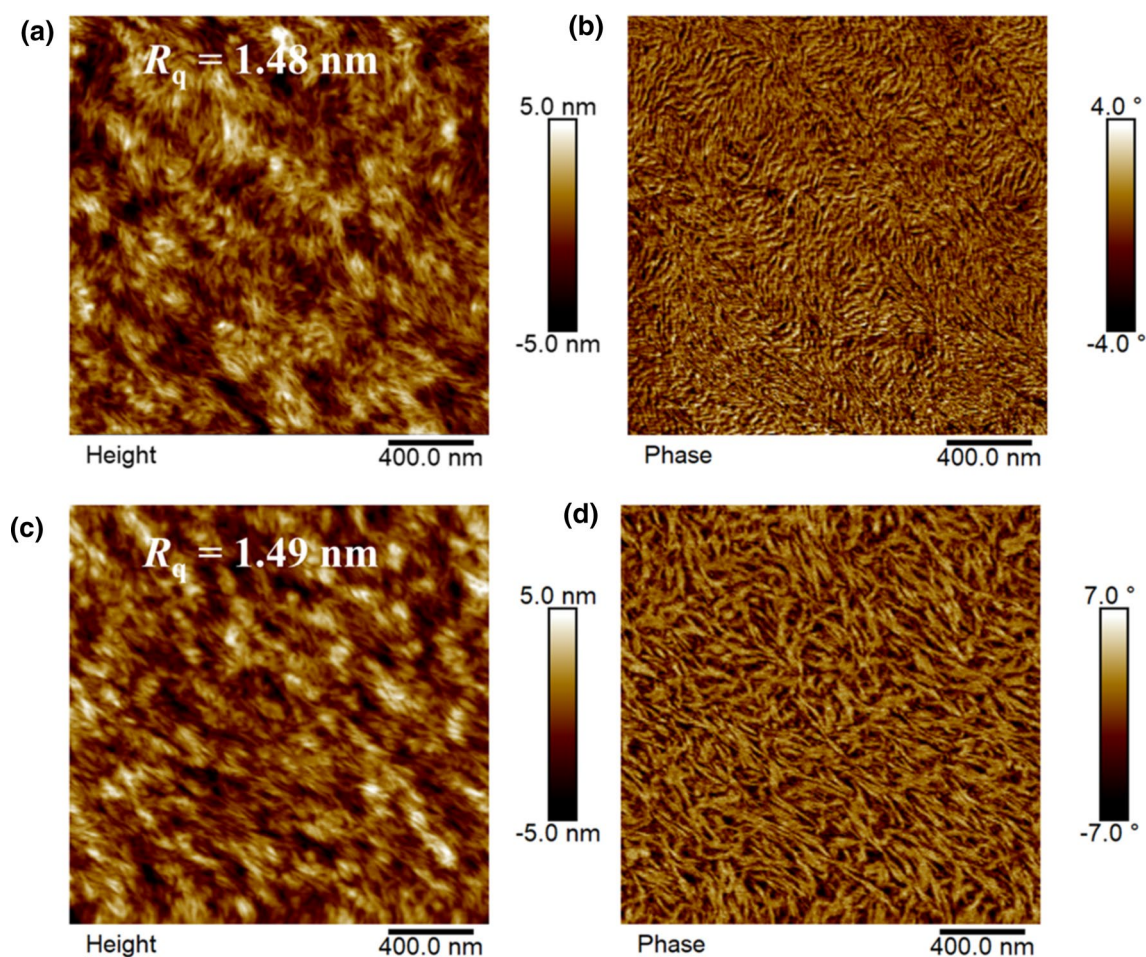


Fig. 8 AFM patterns of the blend films. **a** Height and **b** phase images for PSZ:BTP-eC9 blend; **c** height and **d** phase images for PSZ:PBDB-TF:BTP-eC9 ternary blend film

increased to 0.85 V, and the output efficiency reached 17.4%. These results indicate that thiazole units have great potential application in designing highly efficient photovoltaic materials with low-lying energy levels.

Acknowledgements This work is supported by the National Natural Science Foundation of China (Nos. 22122905 and 22075301).

Declarations

Conflict of interest The authors declare that there are no conflicts of interest.

Open Access This article is licensed under a Creative Commons Attribution 4.0 International License, which permits use, sharing, adaptation, distribution and reproduction in any medium or format, as long as you give appropriate credit to the original author(s) and the source, provide a link to the Creative Commons licence, and indicate if changes were made. The images or other third party material in this article are included in the article's Creative Commons licence, unless indicated otherwise in a credit line to the material. If material is not included in the article's Creative Commons licence and your intended use is not

permitted by statutory regulation or exceeds the permitted use, you will need to obtain permission directly from the copyright holder. To view a copy of this licence, visit <http://creativecommons.org/licenses/by/4.0/>.

References

1. Huang F, Bo Z, Geng Y et al (2019) Study on optoelectronic polymers: an overview and outlook. *Acta Polymerica Sinica* 50(10):988–1046
2. Cui Y, Xu Y, Yao HF et al (2021) Single-junction organic photovoltaic cell with 19% efficiency. *Adv Mater* 33(41):e2102420
3. Li YF (2012) Molecular design of photovoltaic materials for polymer solar cells: toward suitable electronic energy levels and broad absorption. *Acc Chem Res* 45(5):723–733
4. Zhou KK, Xian KH, Ye L (2022) Morphology control in high-efficiency all-polymer solar cells. *InfoMat* 4(4):e12270
5. Dou CD, Liu J, Wang LX (2017) Conjugated polymers containing B←N unit as electron acceptors for all-polymer solar cells. *Sci China Chem* 60(4):450–459

6. Fan HJ, Zhu XZ (2015) Development of small-molecule materials for high-performance organic solar cells. *Sci China Chem* 58(6):922–936
7. Zeng G, Zhang JW, Chen XB et al (2019) Breaking 12% efficiency in flexible organic solar cells by using a composite electrode. *Sci China Chem* 62(7):851–858
8. Zhang ZG, Li YF (2015) Side-chain engineering of high-efficiency conjugated polymer photovoltaic materials. *Sci China Chem* 58(2):192–209
9. Lin YZ, Wang JY, Zhang ZG et al (2015) An electron acceptor challenging fullerenes for efficient polymer solar cells. *Adv Mater* 27(7):1170–1174
10. Yuan J, Zhang YQ, Zhou LY et al (2019) Single-junction organic solar cell with over 15% efficiency using fused-ring acceptor with electron-deficient core. *Joule* 3(4):1140–1151
11. Zheng Z, Yao HF, Ye L et al (2020) PBDB-T and its derivatives: a family of polymer donors enables over 17% efficiency in organic photovoltaics. *Mater Today* 35:115–130
12. Gao L, Zhang ZG, Xue LW et al (2016) All-polymer solar cells based on absorption-complementary polymer donor and acceptor with high power conversion efficiency of 8.27%. *Adv Mater* 28(9):1884–1890
13. Fan BB, Zhang DF, Li MJ et al (2019) Achieving over 16% efficiency for single-junction organic solar cells. *Sci China Chem* 62(6):746–752
14. Xu Y, Cui Y, Yao HF et al (2021) A new conjugated polymer that enables the integration of photovoltaic and light-emitting functions in one device. *Adv Mater* 33(22):e2101090
15. Cui Y, Yao HF, Hong L et al (2020) Organic photovoltaic cell with 17% efficiency and superior processability. *Natl Sci Rev* 7(7):1239–1246
16. Cui Y, Yao HF, Zhang JQ et al (2020) Single-junction organic photovoltaic cells with approaching 18% efficiency. *Adv Mater* 32(19):e1908205
17. Frisch MJ, Trucks GW, Schlegel HB et al. (2009) Gaussian, Inc., Wallingford, CT, USA
18. Yao HF, Qian DP, Zhang H et al (2018) Critical role of molecular electrostatic potential on charge generation in organic solar cells. *Chin J Chem* 36(6):491–494
19. Cui Y, Yao HF, Hong L et al (2019) Achieving over 15% efficiency in organic photovoltaic cells via copolymer design. *Adv Mater* 31(14):e1808356



His current research interest is establishing rational relationships among molecular structure, aggregation behavior, and photoelectronic performance for organic conjugated systems.



materials.

Huifeng Yao received his PhD from the Institute of Chemistry, Chinese Academy of Sciences (2017), in the group of Prof. Jianhui Hou, studying the molecular design and application of organic photovoltaic materials. He received support from the National Science Fund of China for Excellent Young Scholars in 2022. At present, he has been promoted as an associate researcher in the institute, working on developing feasible molecular strategies for designing highly efficient organic photovoltaic materials.

Jianhui Hou is a professor at ICCAS since 2010 and an adjunct professor at University of Science and Technology Beijing since 2012. He received his Ph.D. degree in physical chemistry from ICCAS in 2006. Then he worked as a postdoctoral researcher in University of California, Los Angeles from 2006 to 2008 and then worked as Director of Research of Solarmer Energy Inc. from 2008 to 2010. His group currently focuses on the design, synthesis, and application of photoelectric